IOPscience iopscience.iop.org

Home Search Collections Journals About Contact us My IOPscience

Pulsed photoconductive antenna terahertz sources made on ion-implanted GaAs substrates

This article has been downloaded from IOPscience. Please scroll down to see the full text article.

2005 J. Phys.: Condens. Matter 17 7327

(http://iopscience.iop.org/0953-8984/17/46/016)

View the table of contents for this issue, or go to the journal homepage for more

Download details:
IP Address: 129.252.86.83
The article was downloaded on 28/05/2010 at 06:47

Please note that terms and conditions apply.

Institute of Physics Publishing — Journal of Physics: Condensed Matter

J. Phys.: Condens. Matter **17** (2005) 7327–7333 doi:10.1088/0953-8984/17/46/016

Pulsed photoconductive antenna terahertz sources made on ion-implanted GaAs substrates

B Salem[1], **D Morris**[1], **V Aimez**[2], **J Beerens**[2], **J Beauvais**[2] **and D Houde**[3]

[1] Regroupement Québécois sur les Matériaux de Pointe, Département de Physique, Université de Sherbrooke, Sherbrooke, QC, J1K 2R1, Canada
[2] Regroupement Québécois sur les Matériaux de Pointe, Département de Génie électrique et Génie informatique, Université de Sherbrooke, Sherbrooke, QC, J1K 2R1, Canada
[3] Regroupement Québécois sur les Matériaux de Pointe, Département de médecine nucléaire et radiobiologie, Université de Sherbrooke, Sherbrooke, QC, J1K 2R1, Canada

E-mail: Bassem.salem@USherbrooke.ca

Received 20 May 2005, in final form 5 October 2005
Published 1 November 2005
Online at stacks.iop.org/JPhysCM/17/7327

Abstract
In this work we show that improved performances of terahertz emitters can be obtained using an ion implantation process. Our photoconductive materials consist of high-resistivity GaAs substrates. Terahertz pulses are generated by exciting our devices with ultrashort near-infrared laser pulses. The ion implantation introduces non-radiative centres, which reduce the carrier lifetime in GaAs. The presence of the charged defects also induces a redistribution of the electric field between the antenna electrodes. This effect has a huge influence on the amplitude of the radiated terahertz field. Results obtained as a function of the laser excitation power are discussed and a comparison of the performance of these devices with a conventional antenna-type emitter is given.

1. Introduction

Terahertz (THz) radiation systems have received much interest in recent years due to their widespread scientific and military applications. The ultra-wide band and the optical coherence of THz pulses also account for considerable efforts made to apply THz technology to spectrally determine the optical and electrical properties of crystals, polymers, and organic liquids. THz radiation has been generated by illuminating various emitters, including externally biased photoconductive (PC) antennas, surface built-in field biased semiconductors, and nonlinear crystals with short optical pulses. In the last decade, low-temperature (LT) grown GaAs [1, 2] has been widely used as the substrate of PC antennas for generation and detection of THz radiation. Such materials can be processed to obtain high resistivity (10^7 Ω cm) [3] and reasonably good carrier mobility (100–300 cm^2 V^{-1} s^{-1}) [2, 4], in addition to short carrier lifetime (<1 ps) [5, 6]. These excellent characteristics are however difficult to reproduce from sample to sample because the quality of the material depends critically on both the

 © 2005 IOP Publishing Ltd Printed in the UK

growth temperature and the post-growth thermal annealing conditions. Recently, an alternative material was reported to be promising as the substrate material of PC antennas, that is, the arsenic ion implanted GaAs (denoted GaAs:As hereafter) [7]. These materials exhibit good structural and electrical properties, and show ultrafast optoelectronic response. It is again possible to improve the carrier mobility of these ion-bombarded materials using post-implanted thermal annealing process. Good control over the overall fabrication process allows studies of the influence of parameters such as the ion implantation dose, the ion energy, and the thermal annealing conditions on the PC antenna characteristics.

GaAs:As PC antennas have been shown to be better terahertz emitters than those made on semi-insulating (SI) GaAs substrates [8–11]. Such enhancement results from ultrafast carrier recombination associated with the presence of the implantation-induced defects. On the other hand, several groups have shown good characteristics of THz emitters with the use of PC antennas made on GaAs substrates grown by the Czochralski method when these devices are photoexcited near the anode. A nonuniform electric field between the electrodes of the antenna, resulting from background charged defects (EL2 defects), might explain this result [12]. Although defects seem to play a crucial role in the characteristics of THz PC antenna emitters, there are very few studies that investigate the role of defects on these characteristics. Ion implantation using other types of ions has already been used successfully to reduce the carrier lifetime in SI GaAs and on III–V semiconductor material in general [13]. For example, subpicosecond lifetime can be obtained in GaAs:H, GaAs:O and GaAs:N [14–16]. However, few papers report fabrication of antennas on such material substrates.

In this paper, we measure the characteristics of PC antenna emitters fabricated on GaAs:As, GaAs:H, GaAs:O and GaAs:N ion-implanted substrates and we compare them with those obtained for a similar emitter fabricated on SI-GaAs substrate. In all cases (except for GaAs:N), we have found better THz integrated intensity for emitters made on ion-implanted substrates. We also show that the implantation-induced defects have an effect on the electrical properties of the antenna and discuss the influence of these defects on the electric field distribution between its electrodes. This paper represents a first step towards a more systematic study of the influence of each implantation parameter on the emission efficiency of pulsed-THz sources made on SI GaAs substrates.

2. Experiment

In this work, we have used commercial high-resistivity ($>10^7$ Ω cm) liquid-encapsulated-Czochralsky-(LEC-) grown, (100)-oriented, semi-insulating (SI) GaAs substrates as starting materials. Our GaAs:As, GaAs:H, GaAs:O and GaAs:N substrates were then prepared using ion implantation at room temperature. For each substrate, multiple implants using different ion energies have been performed. The ion implantation conditions for each substrate studied are summarized in table 1. Note that our low-energy implanter limits the higher ion energy to 180 keV for singly ionized species and to 360 keV for doubly ionized species. After implantation the samples were first capped by GaAs substrate and then annealed at 500 °C for 20 min, with flowing N_2 gas. The number of vacancies per ion generated in the volume of the GaAs matrix is calculated using stopping range of ion in matter (SRIM) software [17]. Results are presented in figure 1. Except for the As ions, our implantation conditions are such that the vacancy distribution profile is relatively flat over the $1/e$ penetration depth of our 760 nm laser excitation beam.

The structure of the photoconductive dipole antenna is shown in figure 2. The electrode pattern is made using a conventional photolithography technique. Ohmic contacts were obtained by using a standard mixture of Ni/Au–Ge/Au for the metallization. The width (W)

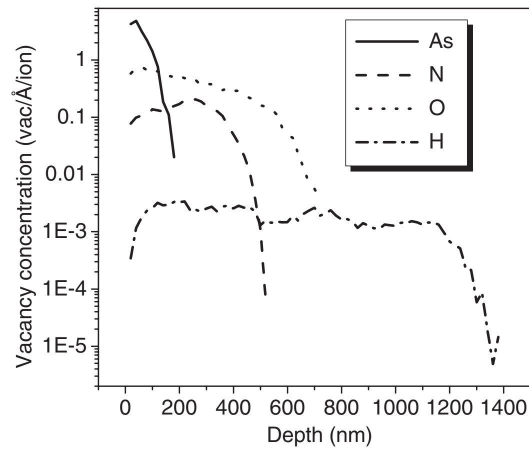

Figure 1. Depth dependence of induced vacancies in GaAs calculated using SRIM software for the As (solid line), N (dashed line), O (dotted line) and H (dash–dot line) ions.

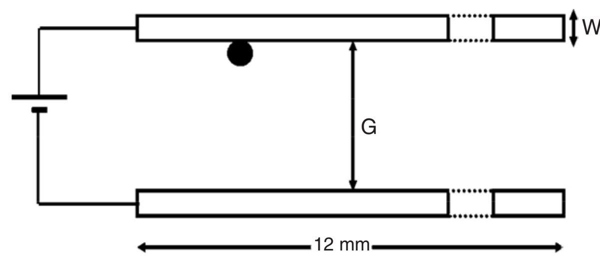

Figure 2. Structure of our photoconductive antenna. The position of the excitation spot is also shown.

Table 1. Ion implantation conditions.

Ion type	Energy (keV)	Doses (cm^{-2})
H	24	2×10^{12}
	60	2.4×10^{12}
	110	3.2×10^{12}
	160	5.2×10^{12}
As	50	2×10^{15}
	100	3×10^{15}
	180	4×10^{15}
O	30	1×10^{11}
	100	2×10^{11}
	200	3×10^{11}
	320	3×10^{11}
N	180	3×10^{14}

of each electrode and the antenna photoconductive gap (G) are 10 and 120 μm, respectively. In order to avoid electromagnetic reflections at the end of the antenna, we are using 12 mm long electrodes.

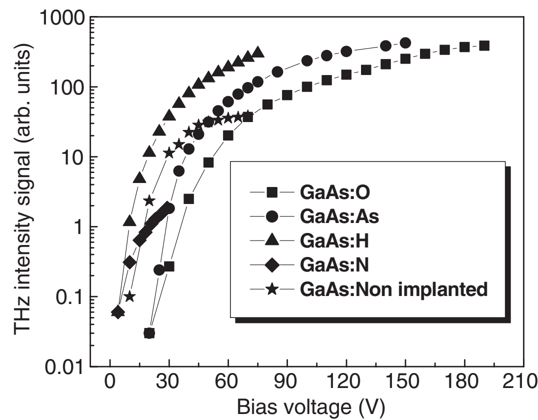

Figure 3. Bias voltage dependence of the THz intensity signal for PC antennas fabricated on SI-GaAs, GaAs:As, GaAs:N, GaAs:H and GaAs:O substrates. The laser excitation beam was focused near the anode (shown in figure 1) and the power was constant at 90 mW.

A mode-locked Ti:sapphire laser at a repetition rate of 82 MHz has been used as the excitation source for the generation of broadband THz radiation. The laser wavelength was centred at 760 nm and the width of the optical pulses was about 100 fs. At 760 nm, the $1/e$ penetration depth of the optical pulses in GaAs is about 500 nm [18]. The excitation beam, at an average power adjustable from 10 μW to 200 mW, was focused on our PC antennas on a spot size of about 10 μm. Most of our results are obtained by focusing the laser beam near the anode of our antennas. Terahertz radiation was collected and refocused on our detector using a pair of off-axis parabolic mirrors. THz intensity signals have been measured using a liquid-He cooled silicon bolometer as a detector.

3. Results

In the photoconductive approach, THz radiation is generated by the acceleration of charges due to an external bias. According to Maxwell's equation, this acceleration results in the generation of an electromagnetic wave, whose electric field amplitude is proportional to the first time derivative of the underlying transient antenna photocurrent.

Figure 3 shows the bias voltage dependence of the THz intensity signals measured for our series of PC antennas using a constant excitation power of 90 mW, with the laser beam focused near its anode. We have measured these THz signals up to a bias level just below the breakdown threshold. In all cases, we observe a quadratic increase of the THz intensity at low biases followed by a saturation regime. The onset value of this saturation regime is correlated with the resistivity of the substrate. Electrical measurements performed on a similar series of antennas show that higher breakdown voltage thresholds ($>$160 V) are obtained for GaAs:As and GaAs:O antennas. Better THz emission intensity can be achieved with these materials using high voltage biasing. It is interesting to note that comparable THz intensity is also measured for the emitter made on GaAs:H material, but at much lower bias voltage. This enhanced emitter efficiency indicates that proton implantation promotes residual impurity compensation which has the effect of increasing both the resistivity of the substrate and the carrier mobility. Moreover, the nature of the induced defects and their distribution might also be different in this material since the implantation conditions are quite different from the ones chosen for the other ions. Finally, we see that the antenna-type emitter made on GaAs:N

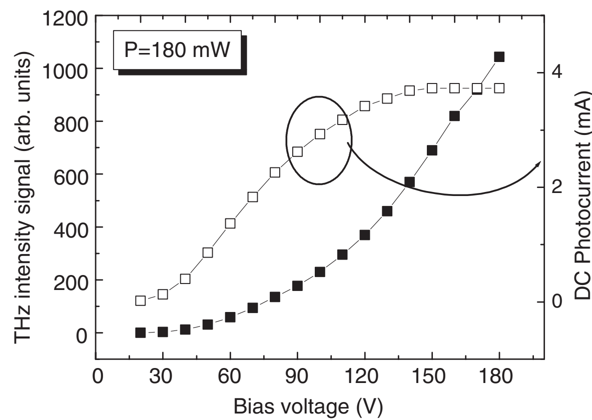

Figure 4. Photocurrent and THz intensity signal as a function of the bias voltage of our PC antenna-type emitter made on GaAs:O substrate. The laser excitation beam was focused near the anode (shown in figure 1) and the power was constant at 180 mW.

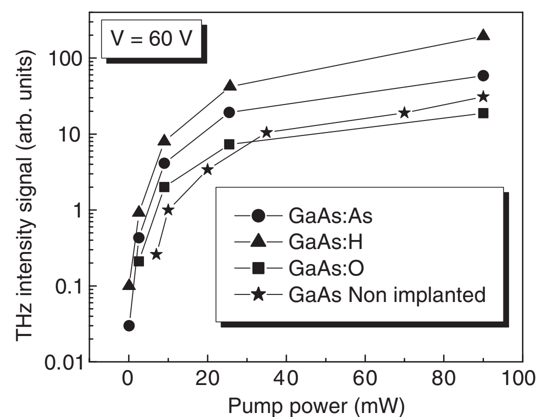

Figure 5. THz intensity signal as a function of laser excitation power for SI-GaAs, GaAs:As, GaAs:N, GaAs:H and GaAs:O PC antenna-type emitters. The bias voltage was constant at 60 V and the laser excitation beam was focused near the anode (shown in figure 1).

material gives less THz signal than the one obtained using an emitter made on non-implanted GaAs substrate. We believe that the nitrogen ions induce defects, which act as dopants, which reduce significantly the resistivity of the GaAs material. These extra free carriers can partially reabsorb the emitted THz radiation.

Figure 4 compares the bias voltage dependence of the THz intensity obtained for the GaAs:O substrate material with its corresponding continuous photocurrent dependence. These results have been obtained for an average laser excitation power of about 180 mW. We see that the onset of the photocurrent saturation regime occurs at a much lower voltage bias than the saturation regime onset of the THz intensity. Similar observations were reported for LT-GaAs PC antenna sources [19]. It seems that the local electric field, which drives the emitted THz radiation, continues to increase with the applied bias even when the DC current starts to saturate due to the enhanced resistivity of the contacts.

Figure 5 shows the laser excitation power dependence of the THz intensity for our emitters made on different substrate materials (except the PC antenna made on GaAs:N, which emits

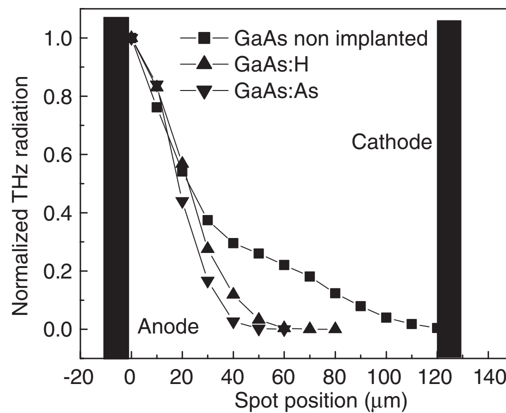

Figure 6. THz intensity signal as a function of the laser spot position between the emitter electrodes. The laser excitation power was constant at 70 mW.

too low THz radiation intensity for accurate measurements) biased at a constant voltage of 60 V. In all cases, we clearly see a saturation regime which occurs at excitation powers greater than 20 mW. This phenomenon originates from the screening of the local bias field by the photocarriers generated in the gap between of our antenna electrodes. It is interesting to note that the onset of this saturation regime does not greatly depend on the substrate material. This result suggests that the dielectric constant of our materials does not vary significantly after the ion implantation treatment.

As observed by several other authors (see, for example, [12]), our devices fabricated on high resistivity GaAs substrates emit stronger THz radiation when the excitation beam is focused near the anode of the antennas. Figure 6 shows the THz intensity signal detected for different laser spot positions between the emitter electrodes. We compare the results obtained for four of our PC antennas excited with a laser beam power of 70 mW. We see a non-linear dependence of the THz intensity signal as a function of the excitation position. These results suggest that the enhanced emission efficiency obtained for our ion-implanted GaAs:H and GaAs:As antennas, excited near their anode, comes from a redistribution of the electric field between their electrodes. The ion implantation process most probably induces defects which act as a background of negative charges. For a uniform distribution of charged defects, the electric field is expected to vary linearly between the electrodes, being higher near the anode side. The nonlinear THz intensity dependence observed in figure 5 must therefore be related to the presence of supplementary negative space charges near the anode. We suggest that these extra charges come from preferential impact ionization of acceptor type defects associated with the acceleration of electrons from the cathode to the anode. The smaller THz intensity slope observed near the anode of our non-implanted GaAs PC antenna (biased at around 50 V) is consistent with the lower THz intensity signal observed in that case (see figure 3).

4. Conclusions

In summary, we have measured the characteristics of a series of PC antenna-type emitters fabricated on either non-implanted or ion-implanted substrates. In all cases, except for the antenna made on GaAs:N substrate, the ion-implantation process allows us to obtain a higher THz radiation intensity in the saturation regime of our emitters. Results obtained for the THz source made on GaAs substrate implanted with protons at relatively low doses (fewer

defects) indicate that it is possible to further improve the efficiency of such pulsed-THz emitters through a better control of the ion-implantation and the thermal annealing conditions. A better knowledge of the nature of the defects and their spatial distributions could help to design optimized materials having short carrier lifetime, high carrier mobility, and the presence of a region of high electric field.

Acknowledgments

This work was supported by FEMTOTECH, an oriented research project supported by Valorisation-Recherche-Québec. It was also supported by NSERC and Nano-Québec. The authors want to thank our technician staff, S Melançon, M Lacerte, P Lafrance, G Bertrand and C Roy, for sample preparation and processing.

References

[1] Tani M, Matsuura S, Sakai K and Nakashima S 1997 *Appl. Opt.* **36** 7853
[2] Tani M, Sakai S and Mimura H 1997 *Japan. J. Appl. Phys.* 2 **36** L1175
[3] Smith F W, Le H Q, Diadiuk V, Hollis M A, Calawa A R, Gupta S, Frankel M, Dykaar D R, Mourou G A and Hsiang T Y 1989 *Appl. Phys. Lett.* **54** 890
[4] Look D C 1993 *Thin Solid Films* **231** 61
[5] Ludwig C and Kuhl J 1996 *Appl. Phys. Lett.* **69** 1194
[6] Kono S, Tani M and Sakai K 2001 *Appl. Phys. Lett.* **79** 898
[7] Claverie A, Namavar F and Liloental-Weber Z 1993 *Appl. Phys. Lett.* **62** 1271
[8] Liu T-A, Tani M and Pan C-L 2003 *J. Appl. Phys.* **93** 2996
[9] Lin G-R and Pan C-L 2001 *Appl. Phys.* B **72** 151
[10] Lloyd-Hughes J, Castro-Camus E, Fraser M D, Jagadish C and Johnston M B 2004 *Phys. Rev.* B **70** 235330
[11] Liu T-A, Tani M, Nakajima M, Hangyo M and Pan C-L 2003 *Appl. Phys. Lett.* **83** 1322
[12] Ralph S E and Grischkowsky D 1991 *Appl. Phys. Lett.* **59** 1972
[13] Pearton S J 1990 *Mater. Sci. Rep.* **4** 313
[14] Lambsdorff M, Kuhl J, Rosenzweig J, Axmann A and Schneider J 1991 *Appl. Phys. Lett* **58** 1881
[15] Lederer M J, Luther-Davies B, Tan H H, Jagadish C, Haiml M, Seigner U and Keller U 1999 *Appl. Phys. Lett.* **74** 1993
[16] Mikulics M, Marso M, Kordos P, Stancek S, Kovác P, Zheng X, Wu S and Sobolewski R 2003 *LLE Review* vol 95, p 192
[17] Ziegler J F and Biersack J P available online at http://www.srim.org
[18] Lush G B, Melloch M R, Lundstrom M S, MacMillan H F and Asher A 1993 *J. Appl. Phys.* **74** 4694
[19] Mendis R, Sydlo C, Sigmund J, Feiginov M, Meissner P and Hartnagel H L 2004 *Solid State Electron.* **48** 2041